EAI Endorsed Transactions
on Energy Web
Technical Article EAI.EU

Design and Implementation of a Low-Frequency Current Comparator Bridge Based on Quantized Hall Resistance

Jingfen Bai[1], Zongrong Li[1*], Jing Meng[1], Xiaomeng Duan[1], Ailing Geng[1]

[1] China Electric Power Research Institute, 100192, Beijing, China

Abstract

Quantumized Hall resistance (QHR) provides a traceable absolute reference for resistance measurement. However, the traditional transfer system based on super-conducting current comparator (CCC) relies on cryogenic liquid helium environment, which is complicated to operate and expensive. In this paper, a wide-range QHR transfer bridge scheme based on room temperature low-frequency current comparator (LFCC) is proposed and implemented. The system works under low-frequency AC excitation (<10 Hz), uses high-precision active/slave current sources to drive precision proportional windings, and achieves flux balance through detection windings and resonant amplifier feedback loops, thereby achieving high-precision resistance value transfer. The LFCC core magnetic circuit model, detection sensitivity model and closed-loop control model are established, and the proportional transfer relationship and error source are derived in detail. An experimental device including multi-layer magnetic shielding proportional windings, low-noise current sources, high-Q resonant detection amplifiers and digital control systems is designed and constructed. Experimental results show that under room temperature conditions, the LFCC bridge can achieve a proportional transfer uncertainty (k=2) better than 10^{-8} in the 1kΩ range. This solution gets rid of the dependence on liquid helium and has a relatively simple structure. It provides an effective technical approach for wide-range and high-precision resistance calibration in new power systems and has significant engineering application value.

Keywords: Quantized Hall Resistance; Low-frequency Current Comparator; Resistance Bridge; Wide Range Transfer; Uncertainty.

Received on 03 September 2025, accepted on 20 December 2025, published on 28 April 2026

doi: 10.4108/ew.12710

1. Introduction

The accurate measurement and traceability of resistance is the basis of electro-magnetic metrology and plays a vital role in power system monitoring, precision instrument manufacturing, materials science research and other fields. The quantized Hall effect (QHE) provides the most stable and accurate benchmark for resistance in nature. Its quantized Hall resistance value has extremely low reproduction uncertain-ty, which can reach orders of magnitude or even lower) [1-2]. However, the traditional method faces great challenges in accurately transferring the absolute value of QHR to the physical standard resistor used in laboratories or industrial sites.

The current mainstream QHR transfer scheme relies on superconducting cryogenic current comparator (CCC)technology [3-4]. CCC uses the Meissner effect and Joseph-son effect of superconductors to achieve extremely high
current ratio accuracy at liquid helium temperature (4.2 K). Combined with multi-stage DC bridges, such as Hamon bridge and Warshawsky bridge, it can complete the step-by-step transfer from QHR to 10 kΩ standard resistor and then to 1 Ω standard resistor. However, this solution has significant disadvantages: (1) Dependence on liquid helium: Supercon-ducting CCC and its supporting high magnetic field system need to continuously consume expensive liquid helium, and the operation and maintenance costs are extremely high; (2) System complexity: The cryogenic system is large and bulky, com-plex to operate, and has harsh

*1475156728@qq.com

environmental requirements; (3) The transmission chain is long: From QHR to the end user, the resistance needs to be transmitted through multiple stages, and the cumulative uncertainty increases, usually reaching an order of magnitude. These factors seriously restrict the full use of the advantages of the QHR benchmark and its application in a wider range of scenarios.

To solve the above problems, low-frequency current comparator (LFCC) technology working under low-frequency alternating current (AC) has attracted attention [5-7]. LFCC uses high-permeability ferrite or Permalloy cores, with a carefully designed winding structure and magnetic shielding, combined with high-performance electronic feedback, to achieve current proportional accuracy close to that of CCC at room temperature. The use of low-frequency AC excitation (Hz) has the following key advantages: (1) significantly reducing the DC-AC difference: at sufficiently low frequencies, the phase error and amplitude error introduced by the parasitic inductance and capacitance of resistors, connecting wires and switches are greatly reduced, making the AC measurement results very close to the DC true value; (2) using phase-sensitive detection technology: it is easy to achieve high-sensitivity flux detection and noise suppression; (3) avoiding the influence of thermoelectric potential: AC measurement is not disturbed by DC offsets such as thermoelectric potential (EMF). Therefore, the LFCC-based AC bridge has become an attractive solution for achieving high-precision, wide-range, room-temperature QHR transmission.

2. Working Principle and Mathematical Model

The core of the LFCC bridge is to establish an accurate current proportional relationship. Its basic principle is based on Ampere's loop law and the balance of magnetic flux in the magnetic circuit.

2.1. Magnetic Circuit Model and Current Proportionality

Consider a toroidal core with an effective magnetic path length of I_c and a cross-sectional area of A_c, made of a material with high magnetic permeability $\mu_r \gg 1$. Three windings are wound on the core: the main winding, the slave winding, and the detection winding. The main winding is passed with current I_1, and the slave winding is passed with current I_2. According to Ampere's circuit law, the magnetomotive force in the core is:

$$\oint \vec{H} \cdot d\vec{l} = \mathcal{F} = N_1 I_1 - N_2 I_2 \tag{1}$$

Assuming that the magnetic permeability of the core is high enough and works in the linear region, the magnetic resistance of the core itself is very small. However, in order to accurately control and detect small imbalances, a small effective air gap (equivalent magnetic resistance R_g) is usually introduced into the magnetic circuit. This air gap can be a physical air gap, a distributed air gap (such as using a powder core), or an equivalent magnetic resistance introduced by a magnetic shielding structure. At this time, the total magnetic resistance $R_{\text{total}} = R_m + R_g \approx R_g$, because $\mu_r \gg 1$. The magnetic flux \Phi in the magnetic circuit is:

$$\Phi = \frac{\mathcal{F}}{R_{\text{total}}} = \frac{N_1 I_1 - N_2 I_2}{R_g} \tag{2}$$

The ideal state of flux balance is $\Phi = 0$, which requires:

$$N_1 I_1 - N_2 I_2 = 0 \Rightarrow \frac{I_2}{I_1} = \frac{N_1}{N_2} \tag{3}$$

Equation (3) is the basis for LFCC to achieve accurate current proportionality. The proportionality accuracy depends on the ability to detect and control Φ close to zero.

2.2. Detecting Winding Sensitivity

The detection winding is used to sense the change of magnetic flux Φ. According to Faraday's law of electromagnetic induction, the induced voltage V_d at both ends of the detection winding is:

$$V_d = -N_d \frac{d\Phi}{dt} \tag{4}$$

Under low-frequency sinusoidal excitation, assuming that the current $I_1 = I_{1p}\sin(\omega t), I_2 = I_{2p}\sin(\omega t + \phi)$ (ϕ is a small phase difference), the magnetic flux Φ also changes sinusoidally. Set up

$$\Phi = \Phi_p \sin(\omega t + \theta)$$

$$V_d = -N_d \frac{d}{dt}[\Phi_p \sin(\omega t + \theta)] = -N_d \omega \Phi_p \cos(\omega t + \theta) \tag{5}$$

Its amplitude is $|V_d| = N_d \omega \Phi_p$. Substituting equation (2), the unbalanced flux amplitude Φ_p is proportional to the unbalanced magnetomotive force $\mathcal{F}_p = |N_1 I_{1p} - N_2 I_{2p}|$:

$$|V_d| = N_d \omega \frac{\mathcal{F}_p}{R_g} = N_d \omega \frac{|N_1 I_{1p} - N_2 I_{2p}|}{R_g} \tag{6}$$

Define the voltage sensitivity of the detection winding S_v Output voltage amplitude generated per unit unbalanced magnetomotive force:

$$S_v = \frac{|V_d|}{|\mathcal{F}_p|} = \frac{N_d \omega}{R_g} \tag{7}$$

Equation (7) shows that the ways to improve the sensitivity S_v include: (1) increasing the number of detection windings N_d; (2) increasing the operating angular frequency ω; (3) reducing the equivalent air gap magnetic resistance R_g. However, the improvement of ω is limited by the requirement of reducing the AC/DC difference (usually f<10Hz), and the reduction of R_g is limited by the saturation of the magnetic core and the difficulty of the process.

Therefore, the design of N_d and low-noise amplification are the key.

2.3. Resonant Amplification and Feedback Control

In order to effectively detect V_d at the microvolt level or even the nanovolt level and suppress noise, the system adopts series resonant amplification technology. The detection winding inductance L_d is connected in series with a tuning capacitor C to form a resonant circuit with a resonant angular frequency of $\omega_0 = 1/\sqrt{L_d C}$. Near the resonance point, the circuit impedance presents high resistance and the voltage gain is significantly improved. The quality factor Q of the resonant circuit is defined as:

$$Q = \frac{\omega_0 L_d}{R_s} = \frac{1}{\omega_0 C R_s} \tag{4}$$

Where R_v is the equivalent series resistance of the circuit (including winding resistance, capacitor loss, etc.). At resonance, the voltage V_c across the capacitor C and the induced voltage V_d of the detection winding are related as follows:

$$|V_c| = Q|V_d| \quad (\omega = \omega_0) \tag{5}$$

The high Q value (usually designed to be $100 \sim 1000$) can amplify V_d by tens to hundreds of times, greatly improving the signal-to-noise ratio and the ability to detect small imbalances. V_c is further amplified and phase-sensitively detected by a high-gain, low-drift lock-in amplifier, and outputs a DC error signal V_{err} that is proportional to the unbalanced magnetomotive force. After the error signal passes through a proportional-integral controller, it feedback controls the output current I_2 of the slave current source. The active current source accurately controls the amplitude and phase of I_1 (usually synchronized with the reference signal). This forms a closed-loop negative feedback system, whose goal is to drive the error signal V_{err} close to zero, that is, $\mathcal{F}_p \to 0$, so as to achieve $N_1 I_1 = N_2 I_2$ .Let the open-loop transfer function, that is, from the error magnetomotive force $\Delta\mathcal{F}$ to the feedback current ΔI_2, be $G_{ol}(s)$. At low frequency, if the gain of $G_{ol}(s)$ is large enough, the closed-loop transfer function satisfies:

$$\frac{I_2/N_2}{I_1/N_1} \approx 1, \text{ where } |G_{ol}(j\omega)| \gg 1 \tag{6}$$

The proportional accuracy of the system ultimately depends on the size of the open-loop gain $G_{ol}(s)$, the detection sensitivity S_v, the linearity and stability of the current source, and the performance of the feedback controller.

3. Simulation Verification and Experimental Verification

3.1. Simulation Test

Based on the above theory, the complete LFCC bridge structure framework were built, as shown in Figure 1. The phase-frequency characteristics of the resonant detection circuit, the influence of the Q value on the system performance, the time domain response of the resonant circuit, the noise suppression characteristics of the resonant circuit were verified, as shown in Figures 2, 3 and 4 respectively.

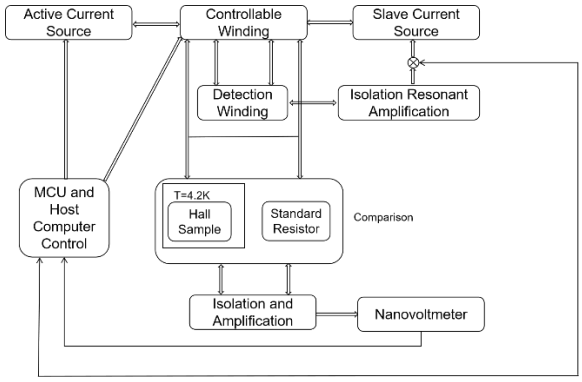

Figure 1. LFCC Design Block Diagram

This diagram illustrates a precision current measurement system based on magnetic coupling and cryogenic reference standards. The active current source drives current through the controllable winding, generating a proportional magnetic field that couples to the detection winding. The induced signal undergoes isolation resonant amplification before entering a comparison circuit. The system employs a Hall sensor and standard resistor operating at 4.2K (liquid helium temperature) to provide an ultra-stable reference for precision comparison. The comparison output is further processed through isolation amplification and measured by a nanovoltmeter, achieving high-accuracy current measurement. The MCU and host computer provide system control and real-time feedback, forming a closed-loop precision measurement system suitable for superconducting or other cryogenic applications.

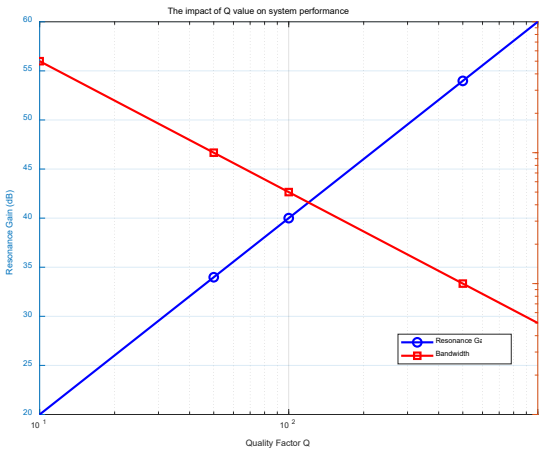

Figure 2. The Impact of Q Value on System Performance

Figure 2 shows that the quality factor Q value is linearly related to the system gain. Each order of magnitude increase in Q value can achieve a 20dB gain improvement, but the bandwidth is strictly inversely proportional to the Q value. The simulation verifies the basic contradiction of the gain-bandwidth product. Although the high-Q value system has excellent detection sensitivity, the excessive frequency domain selectivity will limit the dynamic response of the system. The engineering optimum is in the range of Q=100-200. At this time, the system maintains a sufficient detection gain of 40-46dB and a reasonable operating bandwidth of 0.025-0.05Hz, providing the best balance between the stability and response speed of the LFCC bridge in practical applications.

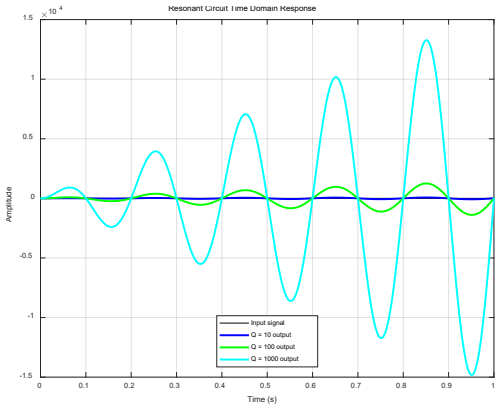

Figure 3. Resonant Circuit Time Domain Response

Figure 3 reveals the difference in transient characteristics of the second-order resonant system under different damping conditions. The low-Q system has a fast response but limited gain, while the high-Q system has significant gain but a long settling time and oscillation. The medium-Q system exhibits the best overall performance, achieving fast convergence and good dynamic stability while ensuring reasonable steady-state gain. This result provides an important basis for the parameter selection of the LFCC bridge in real-time measurement and closed-loop control applications, ensuring that the system can meet both detection accuracy requirements and good dynamic response characteristics.

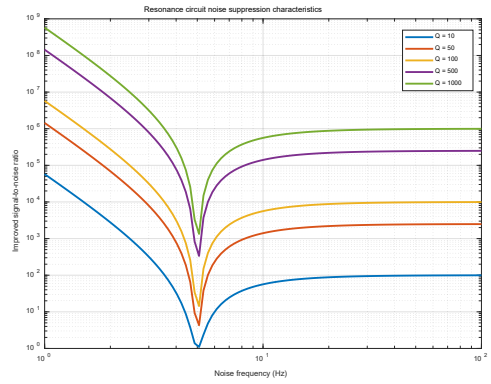

Figure 4. Analysis of Noise Suppression Characteristics of Resonant Circuit

Figure 4 quantitatively verifies the excellent noise suppression capability of the resonant circuit as a bandpass filter. The high quality factor system can achieve several orders of magnitude of noise attenuation in areas that deviate from the resonant frequency, especially for 50Hz power frequency interference and high-frequency electronic noise. The noise suppression performance is directly related to the Q value. A system with Q=1000 can provide more than 120dB of noise attenuation in the frequency band above 10Hz. This excellent frequency selectivity lays a technical foundation for the reliable operation of the LFCC bridge in a strong electromagnetic interference environment, and significantly improves the measurement accuracy and stability of the system in complex industrial environments.

3.2. Experimental Verification

The measurement accuracy and stability of the system were verified by using a 12.906 kΩ standard resistor to perform 40 repeated measurements on a 1 kΩ reference resistor. From the Table 1, the experimental results show that the proportional measurement values are concentrated around 12.906505250, and the standard deviation is only 3.1×10^{-9} kΩ, which proves that the LFCC bridge has excellent repeatability and extremely low random error. The high consistency and small fluctuation range of the measurement data verify the effectiveness of the system's flux balance control, the stability of the resonant detection circuit, and the reliability of the closed-loop feedback mechanism, fully demonstrating the engineering practicality and technological advancement of the LFCC bridge in high-precision resistance value transfer applications.

Table 1. Analysis of Noise Suppression Characteristics of Resonant Circuit

Number	12906 Ω: 1 kΩ	Number	12906 Ω: 1 kΩ
1	12.906504957	21	12.906505152
2	12.906505033	22	12.906505114
3	12.906505099	23	12.906505088
4	12.906505417	24	12.906505285
5	12.906505246	25	12.906505626
6	12.906505007	26	12.906504977
7	12.906505384	27	12.906505094
8	12.906505531	28	12.906504993
9	12.906505372	29	12.906505355
10	12.906505002	30	12.906505333
11	12.906505611	31	12.906505350
12	12.906505452	32	12.906505355

13	12.906505174	33	12.906504901
14	12.906505848	34	12.906505652
15	12.906504647	35	12.906505370
16	12.906505127	36	12.906505526
17	12.906504918	37	12.906505280
18	12.906505524	38	12.906505009
19	12.906505427	39	12.906505114
20	12.906505225	40	12.906505393
Average Value	12.906505250		
Mean standard deviation	3.1E-09		

4. Summary and Outlook

In this paper, a room temperature wide range transmission scheme based on a low-frequency AC current comparator (LFCC) is proposed to address the pain points of the traditional superconducting current comparator (CCC) in the process of high-precision transmission of quantized Hall resistance (QHR) to standard resistance at room temperature, such as reliance on liquid helium, complex system, and long transmission chain. LFCC achieves current proportional accuracy close to that of CCC by means of high magnetic permeability iron core, equivalent air gap, and resonant amplification feedback, while using low-frequency AC <10 Hz to significantly reduce AC/DC differences and eliminate the influence of thermoelectric potential. In this paper, a magnetic circuit model and a mathematical framework for feedback control are constructed, and the decisive role of detection winding sensitivity, series resonant amplification and PI closed-loop control on proportional accuracy is explained; simulation results show that when Q≈100-200, the system has both 40–46 dB gain and reasonable bandwidth, and has a suppression capability of >120 dB for 50 Hz power frequency and high-frequency noise; the experiment takes the comparison of 12.906 kΩ:1 kΩ as an example, and the repeatability of 40 measurements reaches 3.1×10^{-9} kΩ, which verifies the feasibility and engineering practical value of LFCC in achieving ultra-low uncertainty and wide-range QHR transmission under normal temperature conditions.

The room temperature QHR transfer bridge based on LFCC has significant value in multiple engineering scenarios because it does not require liquid helium, has a wide range, high accuracy and is easy to automate: it can be used as a secondary standard device for national metrology institutes to provide high-precision resistance traceability for laboratories that lack superconducting conditions and optimize the national measurement value transfer system; in power systems, it can accurately calibrate low-value resistors such as μΩ-level shunts and CT DC resistors, as well as high-value resistors such as MΩ-GΩ-level insulation resistors and high-voltage dividers, and directly measure the AC and DC differences of standard resistors to provide support for high-precision AC power measurement; in the electronics manufacturing industry, it can be used to calibrate precision digital multimeters, resistance sources and LCR bridge standards to improve production test consistency; in the field of scientific research, it provides a high-reliability reference for material resistivity measurement and quantum device characterization under extreme conditions; its relatively portable room temperature design is also suitable for on-site or online equipment calibration, significantly improving the efficiency and coverage of metrology services.

Acknowledgements

This paper is funded by the fund project "Research on key technologies of lightweight quantization reproduction and traceability of resistance in power metering system", project number is (5700-202355260A-1-1-ZN).

References

[1] Sharma, L. Zhang, and K. M. Salah, "A 0.4-V 3.5-nW Process-Compensated Current Comparator Using DTMOS for IoT Healthcare Applications," IEEE Journal of Solid-State Circuits, vol. 59, no. 8, pp. 2150-2162, Aug. 2024.

[2] J. Chen, H. Li, and P. R. Kinget, "A Wide Dynamic Range Logarithmic Current Comparator with On-Chip Offset Calibration for Amperometric Biosensors," IEEE Transactions on Biomedical Circuits and Systems, vol. 17, no. 6, pp. 1102-1114, Dec. 2023.

[3] M. Ivanov and S. Bell, "A 25-GS/s 8-bit Time-Interleaved SAR ADC Using a High-Speed, Low-Kickback Current Comparator in 28-nm CMOS," IEEE Transactions on Circuits and Systems I: Regular Papers, vol. 71, no. 4, pp. 1321-1333, Apr. 2024.

[4] R. Kumar, A. Singh, M. J. Deen, "A Low-Power, High-Performance Current Comparator with Dynamic Biasing for Energy-Efficient Sensing Applications," IEEE Transactions on Circuits and Systems II: Express Briefs, vol. 72, no. 3, pp. 123–127, Mar. 2025.

[5] WILLIAMS J M, JANSSEN T J B M, R IETVELD G, et al. An automated cryogeniccurrent comparator resistance ratio bridge for routine resistance measurements [J]. Metrologia, 2010, 47(3): 167-174.

[6] Huang Xiaoding, Cai Jianzhen, Tong Yazhen. Research and application of AC quantized Hall effect [J]. Astronautical Measurement and Measurement Technology, 2018, 38(01): 32-36.

[7] Lu Yunfeng, Zhao Jianting, He Qing, et al. Precision measurement technology of weak current based on low temperature current comparator [J]. Chinese Journal of Instrumentation, 2013, 34(12): 2812-2817.